micromachines

Article

Electrical Characterizations of Planar Ga_2O_3 Schottky Barrier Diodes

Shiyu Zhang [1], Zeng Liu [1,2,3], Yuanyuan Liu [4,5], Yusong Zhi [1], Peigang Li [1,*], Zhenping Wu [1] and Weihua Tang [1,2,3,*]

[1] Laboratory of Information Functional Materials and Devices, School of Science & State Key Laboratory of Information Photonics and Optical Communications, Beijing University of Posts and Telecommunications, Beijing 100876, China; zhangshiyu626@163.com (S.Z.); zengliu@bupt.edu.cn (Z.L.); yusongzhi@bupt.edu.cn (Y.Z.); zhenpingwu@bupt.edu.cn (Z.W.)

[2] College of Electronic and Optical Engineering & College of Microelectronics, Nanjing University of Posts and Telecommunications, Nanjing 210023, China

[3] National and Local Joint Engineering Laboratory for RF Integration and Micro-Packing Technologies, Nanjing University of Posts and Telecommunications, Nanjing 210023, China

[4] Center of Materials Science and Optoelectronics Engineering, University of Chinese Academy of Sciences, Beijing 100049, China; liuyy@semi.ac.cn

[5] The Engineering Research Center for Semiconductor Integrated Technology, Institute of Semiconductors, Chinese Academy of Sciences, Beijing 100083, China

* Correspondence: pgli@bupt.edu.cn (P.L.); whtang@bupt.edu.cn (W.T.)

Abstract: In this work, a Schottky barrier diode (SBD) is fabricated and demonstrated based on the edge-defined film-fed grown (EFG) Ga_2O_3 crystal substrate. At the current stage, for high resistance un-doped Ga_2O_3 films and/or bulk substrates, the carrier concentration (and other electrical parameters) is difficult to be obtained by using the conventional Hall measurement. Therefore, we extracted the electrical parameters such as on-state resistance (R_{on}), Schottky barrier height (ϕ_B), the ideal factor (n), series resistance (R_s) and the carrier concentration (N_d) by analyzing the current density–voltage (J–V) and capacitance–voltage (C–V) curves of the Ga_2O_3-based SBD, systematically. The detailed measurements and theoretical analysis are displayed in this paper.

Keywords: Ga_2O_3; Schottky diode; I–V; C–V

Citation: Zhang, S.; Liu, Z.; Liu, Y.; Zhi, Y.; Li, P.; Wu, Z.; Tang, W. Electrical Characterizations of Planar Ga_2O_3 Schottky Barrier Diodes. *Micromachines* **2021**, *12*, 259. https://doi.org/10.3390/mi12030259

Academic Editors: Hieu Pham Trung Nguyen and Henrique Leonel Gomes

Received: 23 January 2021
Accepted: 1 March 2021
Published: 3 March 2021

1. Introduction

Owing to the suitable energy band gap (E_g) of ~4.9 eV, a high Baliga's figure of merit (FOM) of more than 3200, a high Huang's material FOM of 279, Johnson's FOM of 2844, and a high theoretical breakdown field (E_{BR}) of ~8 MV/cm, gallium oxide (Ga_2O_3) has been widely employed to construct optical detectors and power electronics along with low direct current losses and stable operations [1–3]. Till now, Ga_2O_3-based Schottky barrier diodes (SBDs) have achieved high breakdown voltages of 2300 V in a vertical edge-terminated SBD [4] and 3000 V in a lateral field-plated (FP) SBD [5], suggesting strong competitiveness superior to GaN and SiC. Owing to the low dark current and fast response speed [6], the Ga_2O_3-based Schottky diode photodetectors also have drawn much attention for high performances. For instance, the high photo responsivity (R), high external quantum efficiency (EQE), large specific detectivity (D*), and short response time in Ni/β-Ga_2O_3 [7], Pt/ε-Ga_2O_3 [8], graphene/β-Ga_2O_3 [9], and MXenes/β-Ga_2O_3 [10] photodiodes are realized.

In electronic devices, the electrical parameters, such as carrier concentration, are key issues that affect the device design, construction, and operation. For doped Ga_2O_3 and/or the flakes exfoliated from the bulk single crystal, the electron concentrations are reported as 10^{16}–10^{20} cm^{-3} [11–14], while in fact, the un-doped Ga_2O_3 has a high resistance due to the large E_g, thus it is very hard to obtain some electrical parameters via the conventional

Hall measurement. Additionally, a systematic and comprehensive study for electrical characterizations such as on-state resistance (R_{on}), Schottky barrier height (ϕ_B), the ideal factor (n), series resistance (R_s) and the carrier concentration (N_d) of Ga_2O_3 Schottky devices is less reported. Therefore, to solve this problem, we fabricated a Ga_2O_3-based SBD, and then performed the electrical characterizations through the J–V, H(J)–J, and C–V characteristic curves.

2. Experimental Section

The Ga_2O_3 crystal substrate was grown by the edge-defined film-fed grown method, whose scale is 10 mm × 10 mm. For fabricating the Schottky diode, photolithography, lift-off, and electron beam vapor techniques were used to finish the Ni/Au (Schottky, 30 nm/100 nm) and Ti/Au (Ohmic, 30 nm/100 nm) electrode patterns as shown in Figure 1b. X-ray diffraction (XRD), X-ray photoelectron spectroscopy (XPS), and scanning electron microscopy (SEM) were performed to verify the quality of the Ga_2O_3 crystal substrate. The electrical test was executed with Keithley 4200 analysis equipment in the air at room temperature. The area of the electrode pattern is 2.4×10^{-3} cm^2. Figure 1a is the schematic of the planar Ga_2O_3 SBDs.

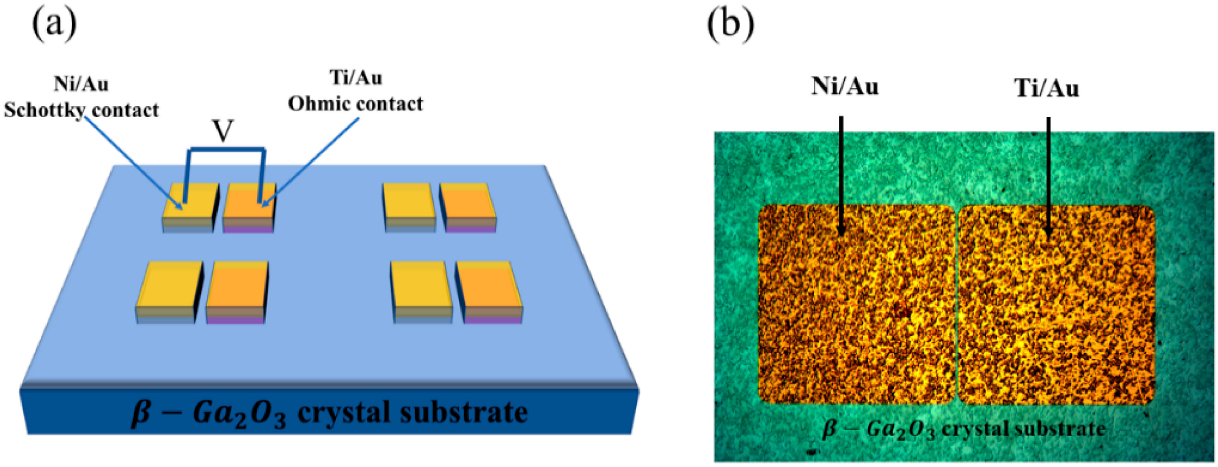

Figure 1. (**a**) The geometry of the Schottky diodes with Ni/$\beta - Ga_2O_3$/Ti structure. (**b**) Optical microscopy image of the fabricated Schottky diode.

3. Results and Discussion

As shown in Figure 2a, the XRD pattern of the edge-defined film-fed (EFG)-grown Ga_2O_3 substrate is displayed, showing (201), (400), (401), (402), and (601) orientations. The prepared Ga_2O_3 crystal is polycrystalline β-Ga_2O_3. The SEM image of the surface of the Ga_2O_3 substrate is portrayed in Figure 2a inset, suggesting a decent crystallization with well-defined boundaries and uniform claviform grains. In Figure 2b, the binding energies of Ga $2p_{1/2}$, Ga $2p_{3/2}$, and O 1s are determined to be 1144.7 eV, 1117.9 eV, and 530.6 eV by XPS, they are similar to the reported values as shown in Table 1, verifying the formation of the Ga_2O_3 semiconductor.

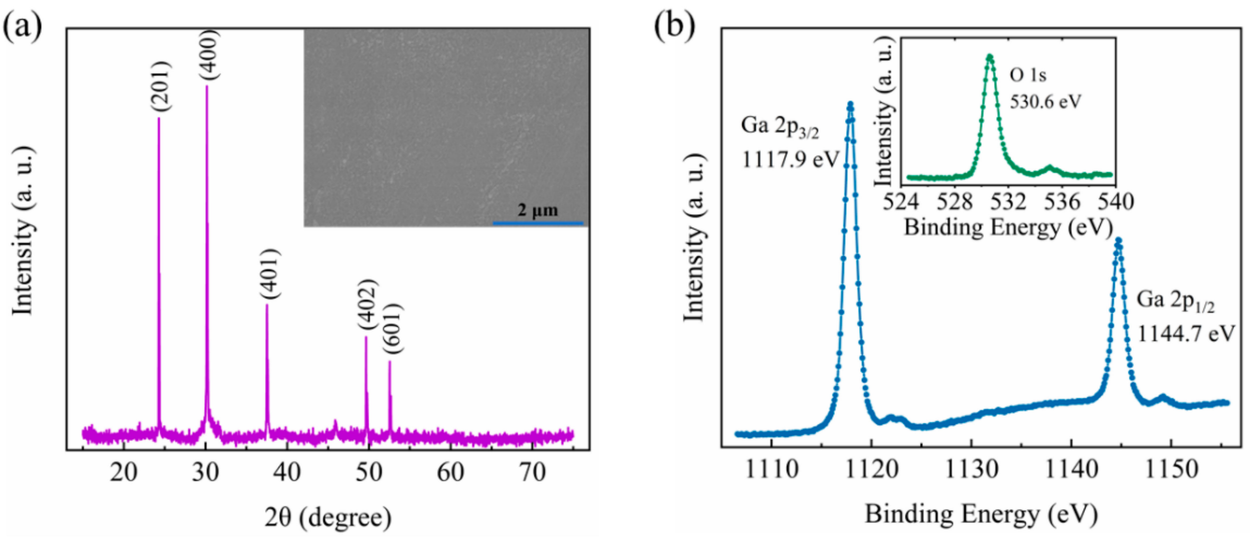

Figure 2. (**a**) The X-ray diffraction (XRD) pattern and (**b**) the X-ray photoelectron spectroscopy (XPS) of the Ga_2O_3 substrate, of which the scanning electron microscope (SEM) image is shown in (**a**) inset.

Table 1. Comparison of the binding energies of Ga $2p_{1/2}$, Ga $2p_{3/2}$, and O 1s.

Ga $2p_{1/2}$ (eV)	**Ga $2p_{3/2}$ (eV)**	**O 1s (eV)**	**Reference**
1144.7	1117.9	530.6	This work
1145.18	1118.28	531.18	[15]
1145	1120	530.7	[16]
1145.5	1118.5	531.4	[17]

In Figure 3a, current density–voltage (J–V) curves of the Ni/Ga_2O_3/Ti Schottky diode are shown in linear-scale and semi-log scale, respectively. The output current density is 3.04×10^{-2} A/cm^2 and 1.25×10^{-7} A/cm^2 at 2 V and -2 V, respectively, translating to a high rectifying ratio of 2.44×10^5; the fabricated device is on-state at forward voltages while off-state at reverse voltages. By extrapolating the linear region of the log-scaled J–V curve in Figure 3a (red line) to obtain its slope, the on-state resistance (R_{on}) is estimated to be 51.5 Ω cm^2. Furtherly, we use the thermionic emission (TE) model to describe the Ni/Ga_2O_3/Ti Schottky diode [18]:

$$J = J_s(e^{\frac{qV}{nkT}} - 1) \tag{1}$$

$$J_s = A^* T^2 e^{-\frac{\phi_B}{kT}} \tag{2}$$

$$\phi_B = \frac{kT}{q} \ln(\frac{A^* T^2}{J_s}) \tag{3}$$

and

$$A^* = \frac{q m^* k^2}{2\pi^2 \hbar^3} \tag{4}$$

where q is the electron charge, V is the applied voltage, J_s is the reverse saturation current, n is the ideal factor, k is the Boltzmann constant, T is the thermodynamic temperature, ϕ_B is the Schottky barrier height, and A^* is the Richardson constant. For Ga_2O_3, its effective electron mass $m^* = 0.342\ m_0$, with m_0 the mass of the free electron, thus the A^* of Ga_2O_3 is calculated to be 41.07 A/cm^2 K^2 [19].

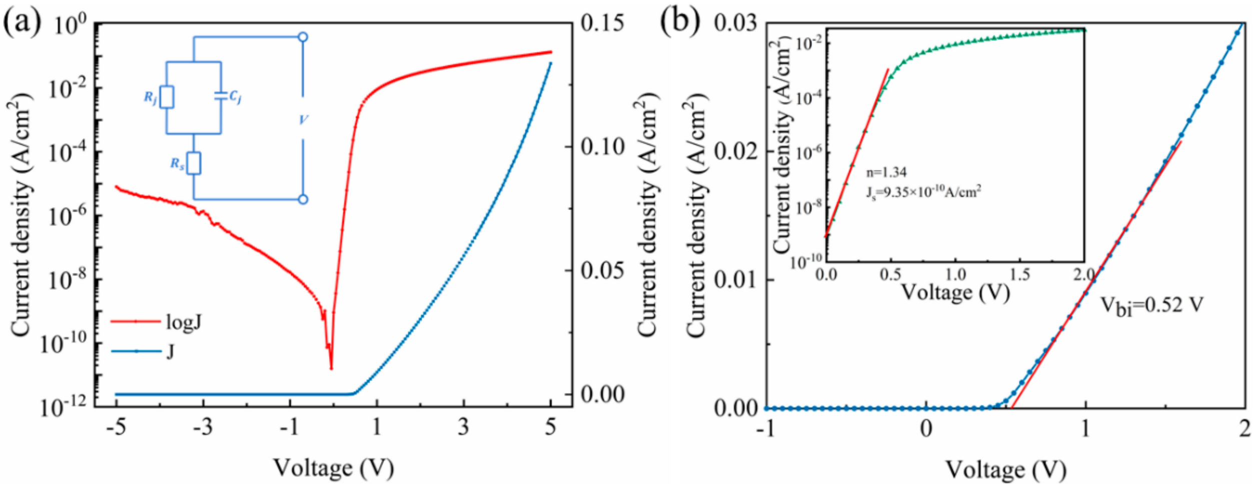

Figure 3. (**a**) The current density–voltage (J–V) curves of the Ni/Ga_2O_3/Ti Schottky diode, inset is the equivalent circuit diagram, (**b**) the n, J_s, and V_{bi} based on thermionic emission (TE) model.

As displayed in Figure 3b, with the TE model described in Equations (1)–(4), the n, ϕ_B and turn-on voltage (V_{on}) are determined to be 1.34, 0.93 eV, and 0.52 V, respectively. In Figure 3b inset, the J_s of the Schottky diode is 9.35×10^{-10} A/cm^2. The n value between 1 and 2, nearer to 1, indicates a decent Schottky electrical behavior in the fabricated device. The V_{on} suggests a built-in potential difference (V_{bi}) of 0.52 eV. In fact, the work function of Ni (W_m) is 5.15 eV [20], and the electron affinity of Ga_2O_3 (χ_s) is 4.00 eV [21]. The Ni-Ga_2O_3 energy band diagram before they make contact is shown in Figure 4a. According to the Schottky–Mott rule [22,23], the Ni-Ga_2O_3 interface barrier is about 1.15 eV, i.e., the difference between W_m and χ_s. After they make contact, as given Figure 4b, the conduction and valence energy band edge (E_c and E_v) bend up, owing to the electron transferring to the electrode. The formation of the ϕ_B indicates a barrier for electron transport in the device, thus the device has a V_{on} and rectifying effect.

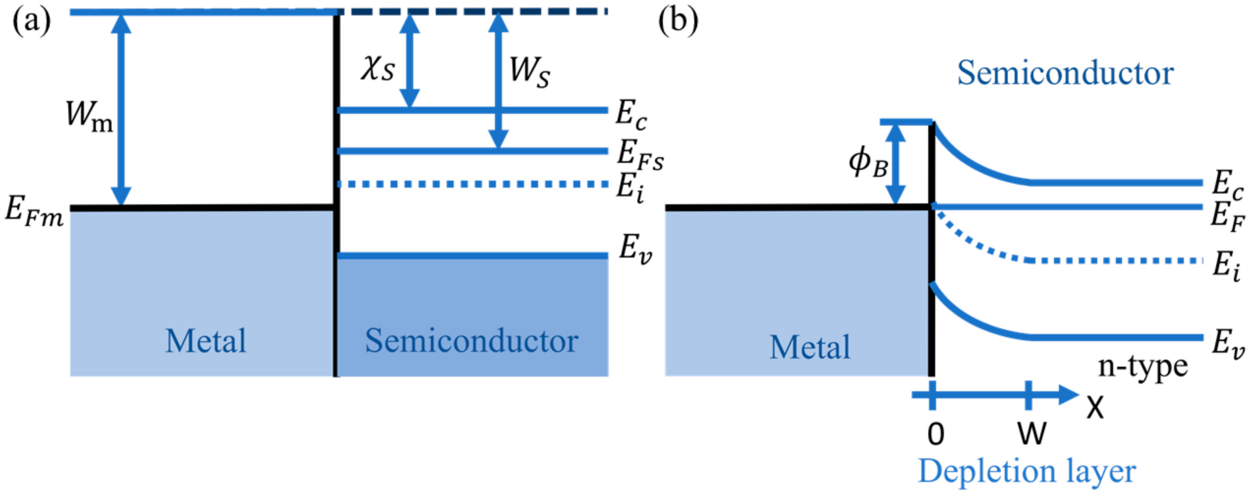

Figure 4. The energy band diagram of the Ni/Ga_2O_3/Ti Schottky diode (**a**) before and (**b**) after contact.

For the device, the series resistance (R_s) is a key parameter affecting the performances of the Schottky diode, modeled by a combination of a capacitance (C_j) and a resistor (R_j) as shown in Figure 2a inset. When the current flow is in the diode, it has a relationship with voltages applied on the device [24]:

$$V_D = V - JAR_s \tag{5}$$

where V_D is the voltage on the two sides of the diode, V is the applied voltage, and A is the area of the electrode. Other than the homojunction device, in the Schottky junction similar to the heterojunction, the key role in determining the electrical behavior could not be told by diffusion current model. When $V_D > 3kT/e$, the current in diode could be described by the thermionic electron model:

$$J = J_s \exp[e(V - JAR_s)/nkT] \tag{6}$$

Thus,

$$V = AR_s J + n\phi_B + \frac{nkT}{e} \ln\left(\frac{J}{A^* T^2}\right) \tag{7}$$

$$dV/dlnJ = AR_s J + \frac{nkT}{e} \tag{8}$$

moreover, H(J) is defined as

$$\mathrm{H(J)} = \mathrm{V} - \frac{e}{nkT} \ln\left(\frac{J}{A^* T^2}\right) = AR_s J + n\phi_B \tag{9}$$

based on Equation (8), through the linear fitting ($dV/dlnJ$)-J curve shown in Figure 5a (blue dot-line curve), the n and R_s of the Schottky diode are estimated to be 1.67 and 45.5 Ω cm^2. Then, according to the Equation (9), ϕ_B and R_s of the Schottky diode could be obtained as 0.86 eV and 46.6 Ω cm^2, by fitting the H(J)-J curve displayed in Figure 5a (green dot-line curve). In addition, according to the energy band diagram in Figure 3, ϕ_B can be demonstrated as $\phi_B = eV_{bi} + (E_c - E_f)$ [18], where E_c and E_f are the conduction minimum and Fermi level of the Ga_2O_3. $E_c - E_f = kTln(\frac{N_c}{N_d - N_a})$, where N_c is effective state density at conduction band, expressed as $N_c = 2\frac{2\pi m^* kT}{h^2}^{3/2}$, thus the electron concentration of the Ga_2O_3 can be calculated to be 1.04×10^{19} cm^{-3} [25]. What's more, based on the Norde's method [26], a function F(V) is defined as:

$$\mathrm{F(V)} = \frac{V}{2} - \frac{kT}{e} \ln(\frac{J(V)}{A^* T^2}) \tag{10}$$

so, ϕ_B and R_s could be expressed as:

$$\phi_B = F(V_0) + \frac{V_0}{2} - \frac{kT}{e} \tag{11}$$

and

$$R_s = \frac{kT}{eJ(V_0)A} \tag{12}$$

where V_0 is the voltage at the rock bottom of this function, $F(V_0)$ and $J(V_0)$ are the corresponding functions of V_0. As shown in Figure 5b, the V_0 has been marked as 0.45 V. On the basis of Equations (10)–(12), ϕ_B and R_s of the Schottky diode could be obtained as 1.04 eV and 112.1 Ω cm^2.

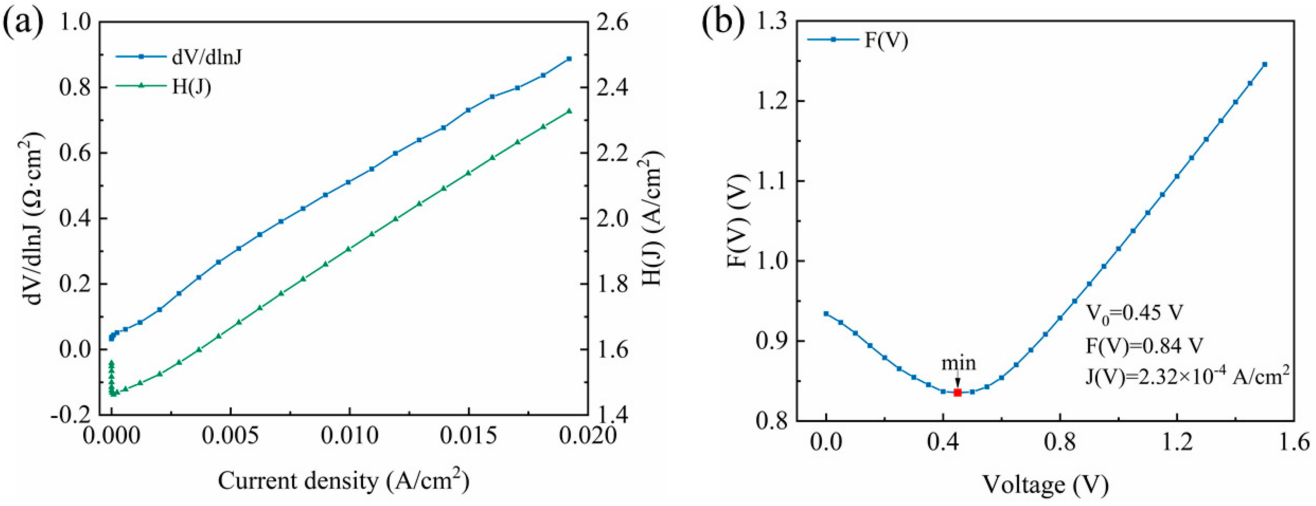

Figure 5. (**a**) The $(dV/dlnJ)$- J and H(J)-J curve, (**b**) F(V)-V curves of the Schottky diode.

The Schottky barrier region in a Schottky diode could be regarded as a planar capacitance, which can be shown as $C = \frac{\varepsilon_s \varepsilon_0 A}{W}$ [25,27], where W is the width of the depletion, ε_s and ε_0 are the permittivity of Ga_2O_3 (ε_s~10) and vacuum permittivity (8.85×10^{-12} F/m). Based on Poisson's equation, it can be described as:

$$\frac{1}{C^2} = \frac{2}{qN_d \varepsilon_s \varepsilon_0 A^2}(V_{bi} - V - \frac{kT}{q}) \tag{13}$$

As shown in Figure 6a, the capacitance–voltage (C–V) and $\frac{1}{C^2}$-V curves are displayed with a frequency (f) of 100 kHz, and it can be clearly seen that the C decreases from 1.75×10^{-10} F to 1.27×10^{-10} F, with a gradual slowing rate. With Equation (13), the N_d could be fitted through the $\frac{1}{C^2}$-V curve to be 4.36×10^{17} cm^{-3}. In addition to Figure 6b, the C is almost unchanged with different frequencies, due to the fact that the current in a Schottky diode is caused by the entrance of a majority carrier into the metal side instead of the charge accumulation, i.e., there is no storage effect, thus no diffusion capacitance. Such characterization is beneficial in constructing high-frequency devices for Ga_2O_3.

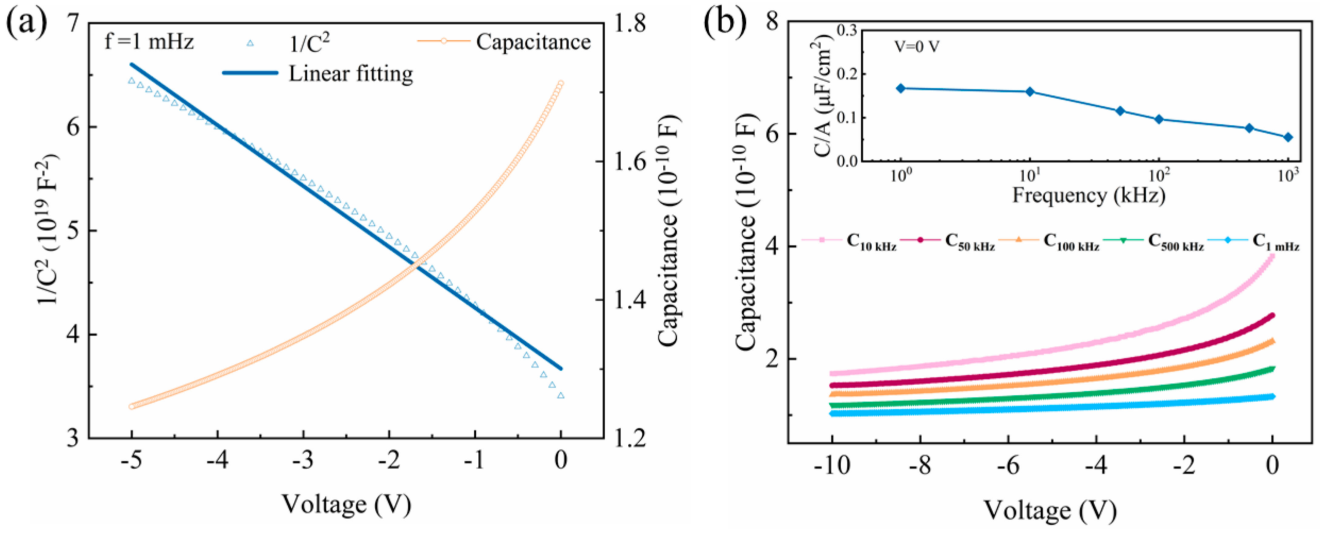

Figure 6. (**a**) The C–V and $\frac{1}{C^2}$-V curves, (**b**) the C–V curves with different frequency.

Table 2 lists and compares the basic electrical parameters of some Ga_2O_3 SBDs in the past two years. From the table, we comprehensively discussed and calculated the basic electrical parameters by different analysis methods of J–V and C–V.

Table 2. Basic performance parameters of some reported Ga_2O_3 Schottky diodes in 2019 and 2020.

Substrate	Anode Metal	V_{br}(V)	$\frac{I_{on}}{I_{off}}$	n	qV_{bi}(eV)	$q\phi_B$(eV)	N_d(cm^{-3})	R_{on} (mΩ·cm^2)	R_s (mΩ·cm^2)	Ref
Wafer (100)	Ni	-	2.44×10^5	1.34	0.52	0.93	4.36×10^{17}	51.5	45.5	This work
Epi layer (001)	Ni	261	-	1.21	0.74	-	1.77×10^{16}	77.3	-	[27]
Wafer $(\bar{2}01)$	Ni	23	2×10^{11}	1.21		1.31–1.64	1.96×10^{18}	1.54	-	[28]
Film (100)	Mo	260	-	-	-	1.55	2×10^{17}	-	-	[29]
Wafer $(\bar{2}01)$	Ni/Pt	-	-	1.14	1.3	1.37	1.45×10^{18}	-	-	[30]
Epi layer (001)	Ni	-	1×10^{10}	1.17	-	1.02	6.9×10^{15}	40	-	[31]

4. Conclusions

In this work, an EFG-grown Ni/Ga_2O_3/Ti Schottky diode is fabricated and characterized. By different analysis methods of J–V and C–V, its electrical parameters such as on-state resistance (R_{on}), Schottky barrier height (ϕ_B), the ideal factor (n), series resistance (R_s) and the carrier concentration (N_d) are obtained and discussed, systematically and comprehensively. The further investigation of Ga_2O_3 materials and devices is in inherent demand due to its excellent properties and the prospect of applications.

Author Contributions: S.Z.: methodology, validation, formal analysis, investigation, writing–original draft. Z.L.: conceptualization, methodology, resources, writing–original draft, funding acquisition. Y.L.: validation, investigation. Y.Z., P.L., Z.W.: project administration, funding acquisition. W.T.: supervision, project administration, funding acquisition. All authors have read and agreed to the published version of the manuscript.

Funding: This work was supported by the National Natural Science Foundation of China (Grant No. 61774019), BUPT Excellent Ph.D. Students Foundation (Grant No. CX2020314), the Fund of State Key Laboratory of Information Photonics and Optical Communications (Beijing University of Posts and Telecommunications, Beijing, China), and the Fundamental Research Funds for the Central Universities, China.

Conflicts of Interest: The authors declare that they have no known competing financial interests or personal relationships that could have appeared to influence the work reported in this paper.

References

1. Liu, Z.; Li, P.; Zhi, Y.; Wang, X.; Chu, X.; Tang, W. Review of gallium oxide based field-effect transistors and Schottky barrier diodes. *Chin. Phys. B* **2019**, *28*, 017105. [CrossRef]
2. Zhang, H.; Yuan, L.; Tang, X.; Hu, J.; Sun, J.; Zhang, Y.; Zhang, Y.; Jia, R. Progress of ultra-wide band-gap Ga_2O_3 semiconductor materials in power MOSFETs. *IEEE Trans. Power Electron.* **2020**, *35*, 5157. [CrossRef]
3. Qin, Y.; Long, S.; Dong, H.; He, Q.; Jian, G.; Zhang, Y.; Hou, X.; Tan, P.; Zhang, Z.; Lv, B.; et al. Review of deep ultraviolet photodetector based on gallium oxide. *Chin. Phys. B* **2019**, *28*, 018501. [CrossRef]
4. Yang, J.; Ren, F.; Tadjer, M.; Pearton, S.J.; Kuramata, A. 2300 V Reverse Breakdown Voltage Ga_2O_3 Schottky Rectifiers. *ECS J. Solid State Sci. Technol.* **2018**, *7*, Q92. [CrossRef]
5. Hu, Z.; Zhou, H.; Feng, Q.; Zhang, J.; Zhang, C.; Dang, K.; Cai, Y.; Feng, Z.; Gao, Y.; Kang, X.; et al. Field-Plated Lateral β-Ga_2O_3 Schottky Barrier Diode With High Reverse Blocking Voltage of More Than 3 kV and High DC Power Figure-of-Merit of 500 MW/cm^2. *IEEE Electron Device Lett.* **2018**, *39*, 1564. [CrossRef]
6. Liang, S.; Sheng, H.; Liu, Y.; Huo, Z.; Lu, Y.; Shen, H. ZnO Schottky ultraviolet photodetectors. *J. Cryst. Growth* **2001**, *225*, 110. [CrossRef]

7. Liu, Z.; Wang, X.; Liu, Y.; Guo, D.; Li, S.; Yan, Z.; Tan, C.-K.; Li, W.; Li, P.; Tang, W. A high-performance ultraviolet solar-blind photodetector based on a β-Ga_2O_3 Schottky photodiode. *J. Mater. Chem. C* **2019**, *7*, 13920. [CrossRef]
8. Qin, Y.; Sun, H.; Long, S.; Tompa, G.S.; Salagaj, T.; Dong, H.; He, Q.; Jian, G.; Liu, Q.; Lv, H.; et al. High-Performance Metal-Organic Chemical Vapor Deposition Grown ε-Ga_2O_3 Solar-Blind Photodetector With Asymmetric Schottky Electrodes. *IEEE Electron Device Lett.* **2019**, *40*, 1475. [CrossRef]
9. Chen, N.; Ma, J.; Li, P.; Xu, H.; Liu, Y. Zero-biased deep ultraviolet photodetectors based on graphene/cleaved (100) Ga_2O_3 heterojunction. *Opt. Express* **2019**, *27*, 8717. [CrossRef]
10. Chen, Y.; Zhang, K.; Yang, X.; Chen, X.; Sun, J.; Zhao, Q.; Li, K.; Shan, C. Solar-blind photodetectors based on MXenes–β-Ga_2O_3 Schottky junctions. *J. Phys. D Appl. Phys.* **2020**, *53*, 48400. [CrossRef]
11. Alema, F.; Hertog, B.; Mukhopadhyay, P.; Zhang, Y.; Mauze, A.; Osinsky, A.; Schoenfeld, W.V.; Speck, J.S.; Vogt, T. Solar blind Schottky photodiode based on an MOCVD-grown homoepitaxial β-Ga_2O_3 thin film. *APL Mater.* **2019**, *7*, 022527. [CrossRef]
12. Ma, N.; Tanen, N.; Verma, A.; Guo, Z.; Luo, T.; Xing, H.G.; Jena, D. Intrinsic electron mobility limits in β-Ga_2O_3. *Appl. Phys. Lett.* **2016**, *109*, 212101. [CrossRef]
13. Zhang, F.; Arita, M.; Wang, X.; Chen, Z.; Saito, K.; Tanaka, T.; Nishio, M.; Motooka, T.; Guo, Q. Toward controlling the carrier density of Si doped Ga_2O_3 films by pulsed laser deposition. *Appl. Phys. Lett.* **2016**, *109*, 102105. [CrossRef]
14. Kang, Y.; Krishnaswamy, K.; Peelaers, H.; Van de Walle, G. Fundamental limits on the electron mobility of β-Ga_2O_3. *J. Phys. Condens. Matter* **2017**, *29*, 234001. [CrossRef] [PubMed]
15. Yadav, M.K.; Mondal, A.; Das, S.; Sharma, S.K.; Bag, A. Impact of Annealing Temperature on Band-alignment of PLD Grown Ga_2O_3/Si (100) Heterointerface. *J. Alloys Compd.* **2019**, *819*, 153502. [CrossRef]
16. Yang, H.; Qian, Y.D.; Zhang, C.; Wuu, D.S.; Talwar, D.N.; Lin, H.H.; Lee, J.F.; Wan, L.Y.; He, K.Y.; Feng, Z.C. Surface/structural characteristics and band alignments of thin Ga_2O_3 films grown on sapphire by pulse laser deposition. *Appl. Surf. Sci.* **2019**, *479*, 1246. [CrossRef]
17. Winkler, N.; Wibowo, R.A.; Kautek, W.; Ligorio, G.; List-Kratochvil, E.J.; Dimopoulos, T. Nanocrystalline Ga_2O_3 films deposited by spray pyrolysis from water-based solutions on glass and TCO substrates. *J. Mater. Chem. C* **2019**, *7*, 69. [CrossRef]
18. Tung, R.T. The physics and chemistry of the Schottky barrier height. *Appl. Phys. Rev.* **2014**, *1*, 011304.
19. He, H.; Orlando, R.; Blanco, M.A.; Pandey, R.; Amzallag, E.; Baraille, I.; Rerat, M. First-principles study of the structural, electronic, and optical properties of Ga_2O_3 in its monoclinic and hexagonal phases. *Phys. Rev. B* **2006**, *74*, 195123. [CrossRef]
20. Eastman, D.E. Photoelectric Work Functions of Transition, Rare-Earth, and Noble Metals. *Phys. Rev. B* **1970**, *2*, 1. [CrossRef]
21. Mohamed, M.; Irmscher, K.; Janowitz, C.; Galazka, Z.; Manzke, R.; Fornari, R. Schottky barrier height of Au on the transparent semiconducting oxide β-Ga_2O_3. *Appl. Phys. Lett.* **2012**, *101*, 132106. [CrossRef]
22. Schottky, W.Z. Halbleitertheorie der Sperrschicht- und Spitzengleichrichter. *Eur. Phys. J. A* **1939**, *113*, 367. [CrossRef]
23. Mott, N.F. The Theory of crystal rectifiers. *Proc. R. Soc. A* **1939**, *171*, 27.
24. Cheung, S.K.; Cheung, N.W. Extraction of Schottky diode parameters from forward current-voltage characteristics. *Appl. Phys. Lett.* **1986**, *49*, 85. [CrossRef]
25. Pierret, R.F. *Semiconductor Device Fundamentals*; Publishing House of Electronics Industry: Beijing, China, 1996.
26. Norde, H. A modified forward IV plot for Schottky diodes with high series resistance. *J. Appl. Phys.* **1979**, *50*, 5052. [CrossRef]
27. Ji, M.; Taylor, N.R.; Kravchenko, I.; Joshi, P.; Aytug, T.; Cao, L.R.; Paranthaman, M.P. Demonstration of Large-Size Vertical Ga_2O_3 Schottky Barrier Diodes. *IEEE Trans. Power Electron.* **2021**, *36*, 41. [CrossRef]
28. Xu, Y.; Chen, X.; Cheng, L.; Ren, F.F.; Zhou, J.J.; Bai, S.; Lu, H.; Gu, S.L.; Zhang, R.; Zheng, Y.D.; et al. High performance lateral Schottky diodes based on quasi-degenerated Ga_2O_3. *Chin. Phys. B* **2019**, *28*, 038503. [CrossRef]
29. Yuan, H.; Su, J.; Guo, R.; Tian, K.; Lin, Z.H.; Zhang, J.C.; Chang, J.J.; Hao, Y. Contact barriers modulation of graphene/β- Ga_2O_3 interface for high-performance Ga2O3 devices. *Appl. Surf. Sci.* **2020**, *527*, 146740. [CrossRef]
30. Li, W.S.; Saraswat, D.; Long, Y.; Kazuki, N.; Jena, D.; Xing, H.G. Near-ideal reverse leakage current and practical maximum electric field in β- Ga_2O_3 Schottky barrier diodes. *Appl. Phys. Lett.* **2020**, *116*, 192101. [CrossRef]
31. Reddy, P.S.; Janardhanam, V.; Shim, K.H.; Reddy, V.R.; Lee, S.N.; Park, S.J.; Choi, C.J. Temperature-dependent Schottky barrier parameters of Ni/Au on n-type (001) β-Ga_2O_3 Schottky barrier diode. *Vacuum* **2020**, *171*, 109012. [CrossRef]